Commun. Comput. Phys.
doi: 10.4208/cicp.290212.240812a

Vol. **14**, No. 2, pp. 276-300
August 2013

Linear Scaling Discontinuous Galerkin Density Matrix Minimization Method with Local Orbital Enriched Finite Element Basis: 1-D Lattice Model System

Tiao Lu[1], Wei Cai[2,3,*], Jianguo Xin[3] and Yinglong Guo[4]

[1] *HEDPS & CAPT, LMAM & School of Mathematical Sciences, Peking University, Beijing 100871, P.R. China.*
[2] *INS, Shanghai Jiaotong University, Shanghai 200240, P.R. China.*
[3] *Department of Mathematics and Statistics, University of North Carolina at Charlotte, Charlotte, NC 28223-0001, USA.*
[4] *School of Mathematical Sciences, Peking University, Beijing 100871, P.R. China.*

Received 29 February 2012; Accepted (in revised version) 24 August 2012

Available online 27 November 2012

Abstract. In the first of a series of papers, we will study a discontinuous Galerkin (DG) framework for many electron quantum systems. The salient feature of this framework is the flexibility of using hybrid physics-based local orbitals and accuracy-guaranteed piecewise polynomial basis in representing the Hamiltonian of the many body system. Such a flexibility is made possible by using the discontinuous Galerkin method to approximate the Hamiltonian matrix elements with proper constructions of numerical DG fluxes at the finite element interfaces. In this paper, we will apply the DG method to the density matrix minimization formulation, a popular approach in the density functional theory of many body Schrödinger equations. The density matrix minimization is to find the minima of the total energy, expressed as a functional of the density matrix $\rho(\mathbf{r},\mathbf{r}')$, approximated by the proposed enriched basis, together with two constraints of idempotency and electric neutrality. The idempotency will be handled with the McWeeny's purification while the neutrality is enforced by imposing the number of electrons with a penalty method. A conjugate gradient method (a Polak-Ribiere variant) is used to solve the minimization problem. Finally, the linear-scaling algorithm and the advantage of using the local orbital enriched finite element basis in the DG approximations are verified by studying examples of one dimensional lattice model systems.

AMS subject classifications: 35Q40, 65N30, 65Z05, 81Q05

Key words: Density functional theory, density matrix minimization, discontinuous Galerkin method, linear scaling method.

*Corresponding author. *Email addresses:* tlu@math.pku.edu.cn (T. Lu), wcai@uncc.edu (W. Cai), jxin@uncc.edu (J. Xin), longlazio1900@gmail.com (Y. Guo)

1 Introduction

In the ab-inito quantum mechanical modelling of many electron system, the density-functional theory together with pseudo-potential approximations has established itself as the method of choice [20], especially through the implementation of Kohn-Sham wave functions. Various numerical methods have been developed to solve the one-electron nonlinear Schrödinger equation for the Kohn-Sham (K-S) wave functions, resulting in a diagonalization of the Hamiltonian of the many electron system [8, 9]. Most of the numerical methods are based on plane waves [20], due to the diagonal representation of the kinetic operator, but at a large computational cost scaling as the cubic power of the size of the system (number of atoms) and with a memory use as second power of the system size. Therefore, for large systems it is imperative to develop numerical methods with a linear scaling complexity both in computational time and memory. The development of linear scaling method usually starts with a 1-D lattice system, where an empirical potential representing those of the nuclear cores of the atoms is stipulated, on which the performance of a numerical method will be tested first. This will be our objective in this paper before we tackle the more difficult nonlinear density functional theory for many electron systems. However, most of the key components of the algorithms will be applicable to the latter case except for the treatment of nonlinearity and exchange-correlation energy.

Linear scaling algorithms for many electron systems have seen much development over last decades in the following areas [12]: Fermi operator expansion method [13], Fermi operator projection method [11], the divide-and-conquer method [26], the density-matrix minimization approach [16], the orbital minimization approach [21], and the optimal basis density-matrix minimization scheme [14]. Also, Galli and Parrinello [7] introduced a plane-wave-based algorithm using localized nonorthogonal wave functions. In the paper of Galli [6], it was pointed out that one of the important characteristics of the $\mathcal{O}(N)$ methods is that the calculation of energy and forces do not require the calculation of the eigen energies/states of the effective single-atom Hamiltonian. There are two popular ways of minimizing the total energy E: density matrix (DM) formulation and localized function (LF) formulation [6]. Within both DM and LF formulations, two basic concepts are introduced to go from an $\mathcal{O}(N^3)$ method to an $\mathcal{O}(N)$ scaling method for the minimization of E. Firstly, in the DM approaches, the idempotency constrain on the density operator, i.e. $\hat{\rho}=\hat{\rho}^2$, is not strictly enforced, and a weaker condition is used instead when minimizing E. In addition, the constraint of N-electron equaling to the trace of the density operator is observed. On the other hand, in the LF approaches the orthonormality condition is not explicitly enforced. Weakening either the idempotency or the orthonormality condition leads to the definition of an energy functional of particle density n or wavefunction ψ, respectively, which is different from the energy functional minimized in conventional approaches, but has the same absolute minimum. Secondly, in the DM frameworks this energy functional is minimized with respect to spatially localized DMs; in the LF approaches, the functional is minimized with spatially localized

single particle orbitals.

In this paper, we mainly address the issue of how to optimally discretize the Hamiltonian energy operator with a finite element basis in the framework of density matrix minimization (DMM). The main goal is to combine the physics-based local orbitals associated with the local atomic behavior of the system and traditional piecewise polynomial finite element basis to discretize the support functions. The latter is used to represent the density operator. The discontinuous Galerkin (DG) approximation method is shown to be able to combine efficiently these two types of functions in the calculation of the kinetic energy operator under the hybrid basis. There are two unique features in this DG framework [1, 5], which can be utilized for faster performance of the nonlinear eigenvalue problems in the K-S DFT theory: (1) Flexibility and locality of DG basis: As the basis for the discontinuous Galerkin method is defined locally over each element, we can enrich the usual polynomial basis by physics-based local wave functions, such as local atomic orbital, Gaussian functions, among others, to reflect the general behavior of the local density profiles around atoms inside a given element K. While the enrichment with local orbital functions captures the main physics of the support functions, the regular polynomial basis will provide correction to possible inaccuracy from a specific selection of local wave functions, thus ensure the convergence of the overall discretization once the mesh is refined or the polynomial order is increased. Such a systematic convergence is lacking if only specially selected local orbitals, such as Gaussian functions, are used. Also, by selecting the correct physics-based local wave functions adjusted iteratively to fit the local properties of the simulated system, the matrix for the discrete Hamiltonian is expected to be reduced significantly, allowing large saving in later iterative solutions for the eigenspaces or energy minimizations. (2) Intrinsic parallelism: In the DG discretization of the K-S equation, where the numerical solutions are "patched" together through appropriately defined numerical fluxes along the shared interface between neighboring elements, the communication is only local to these elements. It is well known that such data exchange allows a high degree of parallel efficiency in implementations.

It is evident to see similarity in philosophy between the use of local orbital enriched finite element basis and that of the augmented plane wave (APW) of Slater [23], who proposed the idea of using radial symmetric orbitals corresponding to the strong nuclear potential within a sphere and plane waves outside the sphere corresponding to a constant potential. Both methods use basis functions adaptive to the physical property of wave functions of the system. The major difference though is that in the APW, the proposed basis function is energy dependent with a required continuity of the basis function at the sphere interface, which defines the so-called muffin-tin potential profile. While, the hybrid basis functions proposed here are general and energy independent, and the DG method, with a guarantied numerical convergence in approximation, combine them at the element interfaces at ease with a correct definition of common flux quantity there, as shown later in the paper. It should be noted that the idea of enriching finite element space is a well established technique in computational mechanics in treating corner singularity [2, 3]. DG approximation to Schrödinger equation has also been used in treat-

ing discontinuous potential in quantum dots [18], in computing the resonant tunnelling diode [25] with special high frequency plane wave functions, and, more recently in a similar attempt to this paper in density functional application, in computing the K-S wave functions using numerically calculated basis functions based on a local Hamiltonian of the system [17].

The rest of the paper is organized as follows. In Section 2, we will review the basic components of density matrix minimization (DMM) method for finding the ground state energy for a many-electron system. Then, in Section 3 the discontinuous Galerkin approximation of the energy functional will be introduced using a local orbital enriched piecewise polynomial finite element basis to approximate the support functions, the latter are used to represent the density matrix. In Section 4, the algorithm detail of DG-DMM algorithm is given for a model 1-D lattice system. In Section 5, numerical tests and linear scaling performance of the DG-DMM is given. Finally, a conclusion is presented in Section 6.

2 Density matrix minimization (DMM) for ground state energy

In the Kohn-Sham (K-S) wave function approach of density functional theory of a N_{el}-electron (N_{el}-even) [15], the K-S wave functions are assumed to be orthogonal and the density operator ρ will have the following matrix form

$$\rho(\mathbf{r},\mathbf{r}')=\sum_{i}^{N}\psi_i^*(\mathbf{r}')\psi_i(\mathbf{r}), \tag{2.1}$$

from which the total energy E_{tot} can be calculated by

$$\begin{aligned}E_{tot}[\{\psi_i\}]=&E_K[\rho(\mathbf{r},\mathbf{r})]+E_{XC}[\rho(\mathbf{r},\mathbf{r})]\\&+\frac{1}{2}\int_{R^3}\int_{R^3}\frac{(\rho-m)(\mathbf{r})(\rho-m)(\mathbf{r}')}{|\mathbf{r}-\mathbf{r}'|}d\mathbf{r}d\mathbf{r}'+E_{PS}[\{\psi_i\}],\end{aligned} \tag{2.2}$$

where the kinetic energy $E_K[\rho(\mathbf{r},\mathbf{r})]$,

$$E_K[\rho(\mathbf{r},\mathbf{r})]=2\sum_i\int_{R^3}d\mathbf{r}\psi_i^*(\mathbf{r})\left(-\frac{\hbar^2}{2m}\nabla^2\right)\psi_i(\mathbf{r})\equiv 2tr[\hat{\rho}\widehat{T}], \tag{2.3}$$

and $\widehat{T}$ is the kinetic energy operator as indicated. $E_{XC}[\rho(\mathbf{r},\mathbf{r})]$ is the exchange-correlation functional, usually calculated by a local density approximation [20], and $m(\mathbf{r})$ and E_{PS} are the nuclear ionic function and the pseudo-potential, which account for the interaction of the valence electrons and the nuclear charges and core electrons [24].

Referred to [14], the ground state can be calculated by minimizing the total energy with respect to the density matrix $\rho(\mathbf{r},\mathbf{r}')$, which is required to satisfy the idempotency condition

$$\hat{\rho}=\hat{\rho}^2, \tag{2.4}$$

namely,

$$\rho(\mathbf{r},\mathbf{r}')=\int_\Omega d\mathbf{r}''\rho(\mathbf{r},\mathbf{r}'')\rho(\mathbf{r}'',\mathbf{r}'), \tag{2.5}$$

where Ω is the computational domain. Also, the total number of electron is maintained by the trace of the density operator with a factor of 2 accounting for the spin of the electrons,

$$N_{el}=2\int_\Omega d\mathbf{r}\rho(\mathbf{r},\mathbf{r}). \tag{2.6}$$

The idempotency constrain (2.4) can be satisfied at convergence of a purification procedure proposed in McWeeny [22], by casting ρ as

$$\rho=3\vartheta*\vartheta-2\vartheta*\vartheta*\vartheta, \tag{2.7}$$

for some auxiliary two-point function $\vartheta(\mathbf{r},\mathbf{r}')$. Here, the asterisk represents the continuum analog of matrix multiplication, i.e.

$$\vartheta*\vartheta(\mathbf{r},\mathbf{r}')\equiv\int_\Omega d\mathbf{r}''\vartheta(\mathbf{r},\mathbf{r}'')\vartheta(\mathbf{r}'',\mathbf{r}'). \tag{2.8}$$

The rational behind (2.7) is that if λ is an eigenvalue of ϑ, then the corresponding eigenvalue of ρ is $f(\lambda)=3\lambda^2-2\lambda^3$. This transformation ensures that if ϑ is close to being idempotent, ρ will be closer to being idempotent due to the $\{0,1\}$-limits of the iteration given by the mapping f. During the process of minimizing E_{tot}, using ρ in the form of (2.7) has the effect of driving the eigenvalues towards zero or unity, namely, ρ is driven towards idempotency. For details of this procedure, refer to Li *et al.* [16].

Next, to achieve the linear scaling of the algorithm, the auxiliary function ϑ is expressed in terms of compact supported functions $\phi_\alpha(\mathbf{r})$ – called *support functions*

$$\vartheta(\mathbf{r},\mathbf{r}')=\sum_{\alpha,\beta}\phi_\alpha(\mathbf{r})L_{\alpha\beta}\phi_\beta(\mathbf{r}'), \tag{2.9}$$

which implies that the density matrix will be in the following form

$$\rho(\mathbf{r},\mathbf{r}')=\sum_{\alpha,\beta}\phi_\alpha(\mathbf{r})K_{\alpha\beta}\phi_\beta(\mathbf{r}'), \tag{2.10}$$

and

$$K=3LSL-2LSLSL, \tag{2.11}$$

where $S_{\alpha\beta}$ is the overlap matrix of the support functions,

$$S_{\alpha\beta}=\int_\Omega d\mathbf{r}\phi_\alpha(\mathbf{r})\phi_\beta(\mathbf{r}). \tag{2.12}$$

Moreover, the kinetic energy through the trace operation becomes

$$E_K[\rho(r,r)]=2\sum_{\alpha,\beta}\int_\Omega d\mathbf{r}\phi_\beta(\mathbf{r})K_{\alpha\beta}\left(-\frac{\hbar^2}{2m}\nabla^2\right)\phi_\alpha(\mathbf{r}). \tag{2.13}$$

The support functions $\phi_\alpha(\mathbf{r})$ will be selected to be nonzero only within localized spatial regions, referred to as *support regions*, and that the matrix elements $L_{\alpha\beta}$ be nonzero only if the corresponding regions are separated by less than a chosen cutoff distance R_{cut}. It is natural to impose these conditions because in general $\rho(\mathbf{r},\mathbf{r}')$ decays to zero as the separation $|\mathbf{r}-\mathbf{r}'|$ goes to infinity. This implies that the calculation will become exact as the cutoff distance and the size of the support regions are increased.

The strategy of density matrix minimization (DMM) algorithm now is to minimize the total energy both with respect to the support functions and with respect to the $L_{\alpha\beta}$ coefficients, subject only to the condition that the number of electrons keeps a required value.

3 Discontinuous Galerkin (DG)-DMM with enriched basis

In the discontinuous Galerkin DMM approach, the support functions in (2.9) will be approximated with piecewise polynomial basis enriched by physics-based local orbitals associated with one-atom Hamiltonian. The latter will make sure the dominant profile of the support functions can be captured by the local orbitals, which could be truncated to a local region around each atom. Meanwhile, the polynomial basis will provide numerical convergence of the hybrid enriched basis by either refining the underlying mesh (*h*-refinement) or raising the degree of the polynomials (*p*-refinement) or a *h*-*p* refinement. It will be clear later that the construction of the numerical fluxes provides the flexibility to employ any type of basis in the DG approximation and allows us to design the DG-DMM approach using both physical intuition and mathematical convergence consideration.

The support regions are chosen to be spherical with radius R_{reg} and are centered on the atoms. Each region is associated with a certain number ν support functions, where ν is the same for all regions. It is important to note that the total number of support functions must be greater than half the number of electrons N_{el}. We use α,β,γ denote the index of support function, k,l denote the index of element and i,j denote the index of basis function in an element. Each support function $\phi_\alpha(\mathbf{r})$ is then represented as

$$\phi_\alpha(\mathbf{r}) = u_\alpha^{lo}(\mathbf{r}) + u_\alpha(\mathbf{r}) = u_\alpha^{lo}(\mathbf{r}) + \sum_{k,j} u_{\alpha,j}^k \varphi_j^k(\mathbf{r}), \tag{3.1}$$

using a hybrid basis, i.e. $u_\alpha^{lo}(\mathbf{r})$ is an analytical local orbital function, possibly localized by truncations, related to one atom Hamiltonian, and is selected to capture the dominant feature of the support function $\phi_\alpha(\mathbf{r})$, while $u_{\alpha,j}^k$ is the coefficients of the usual basis functions $\varphi_j^k(\mathbf{r})$, taken to be polynomials with support only on the element I_k.

In an exact calculation, the kinetic energy E_K would be given by (2.13). We assume that the calculation domain $\Omega = \cup_k I_k$. I_k are non-overlapping elements of the domain Ω. The interior boundary set is $\{S_k\} = \bigcup_k \partial I_k \backslash \partial\Omega$. When we use the periodic boundary condition, the interior boundary is $\{S_k\} = \bigcup_k \partial I_k$.

Due to the discontinuous nature of the representation (3.1) for the support function, a direct evaluation of the Laplacian operator $\phi_\alpha(\mathbf{r})$ will produce a divergent integral. In the usual approach for a discontinuous Galerkin finite element method, the integration over Ω will be split into integration over individual element I_k and, to ensure the continuity of the converged solution as the mesh size is decreased or the degree of polynomial is increased, some type of connection between the DG basis functions in neighboring elements should be introduced. In the DG method introduced by Cockburn and Shu [5], such a connection is achieved by defining a unique numerical flux across the common interface between the elements. The detailed derivation of formulae would be illustrated in Section 4.1.

As the energies E_{ps}, E_H, and E_{xc} are considered as a functional of the electron density $n(\mathbf{r})\equiv\rho(\mathbf{r},\mathbf{r})$ as in DFT, which is simply the trace of the Hamiltonian matrix,

$$n(\mathbf{r})=2\sum_{\alpha\beta}\phi_\alpha(\mathbf{r})K_{\alpha\beta}\phi_\beta(\mathbf{r}). \tag{3.2}$$

The pseudopotential energy is evaluated by multiplying $n(\mathbf{r})$ by the total pseudopotential and integration over the computational domain [24]. (For present purpose, we are working with local pseudopotentials, although the extension to nonlocal pseudopotential is straightforward). The LDA exchange-correlation energy is evaluated similarly by $\int_\Omega n(\mathbf{r})\varepsilon_{xc}[n(\mathbf{r})]d\mathbf{r}$, where $\varepsilon_{xc}(n)$ is the exchange-correlation energy per electron at density n. The Hartree energy is evaluated in reciprocal space using the Fourier components of $n(\mathbf{r})$ obtained by a discrete Fourier transform.

Now, the ground state will be determined by minimizing the total energy with respect to both the support function $\phi_\alpha(\mathbf{r})$ and the $L_{\alpha\beta}$ coefficients, though alternatively, with the electron number held constant. The total energy

$$E_{tot}=2\sum_{\alpha\beta}K_{\alpha\beta}H_{\beta\alpha}=2\mathrm{tr}(KH), \tag{3.3}$$

where $H_{\beta\alpha}=\int_\Omega\phi_\alpha(\mathbf{r})\hat{H}\phi_\beta(\mathbf{r})d\mathbf{r}$. As we are using DG finite element to describe the support function, we would introduce an interior penalty term to make sure the support function to be less continuous. We rewrite the total energy as

$$2\mathrm{tr}(KH)+\frac{a}{h}\sum_\alpha\sum_k\int_{S_k}(\phi_\alpha^+(x)-\phi_\alpha^-(x))^2dx=E_{tot}+E_{tot}^{DG}, \tag{3.4}$$

where a is the penalty parameter, h is the mesh size and $\{S_k\}$ is the set of inner boundary between the elements.

When we are finding the minimization of the total energy with the electron number held constant, we will modify the objective energy function into

$$E_{tot}^{Pen}=2\mathrm{tr}((3LSL-2LSLSL)H)+\mu[N_{el}-2\mathrm{tr}((3LSL-2LSLSL)S)]^2, \tag{3.5}$$

where K is replaced with $(3LSL-2LSLS)$ by applying McWeeny's purification, and the total electron number constraint is handled by the penalty method [19]. Let μ be the penalty parameter, and it can be seen that as $\mu\to+\infty$, the unconstraint minimization problem has the same minimization point as the constraint problem. The analytical expressions for the derivatives $\partial E_{tot}^{Pen}/\partial L_{\alpha\beta}$ is given by

$$\frac{\partial E_{tot}^{Pen}}{\partial L_{\alpha\beta}}=6(SL\tilde{H}+\tilde{H}LS)_{\beta\alpha}-4\left(SLSL\tilde{H}+SL\tilde{H}LS+\tilde{H}LSLS\right)_{\beta\alpha}. \tag{3.6}$$

Here $\tilde{H}=H-2\mu[N_{el}-2\mathrm{tr}((3LSL-2LSLSL)S)]S$. The minimization problem of finding the minimization of (3.5) is solved by using the Polak-Ribiere variant of the conjugate gradient method.

Next, we find the minimum of the total energy with respect to the coefficients $u_{\alpha,j}^{k}$ of the support functions $\phi_\alpha(\mathbf{r})$ with the fixed electron number constraint. We obtain the objective energy function when we are minimizing the total energy with respect to the coefficients of all the DG basis functions for the support functions $\phi_\alpha(\mathbf{r})$, which is $\mathbf{u}=\left(u_{00}^{0},u_{01}^{0},\cdots,u_{\alpha j}^{k},\cdots\right)^{T}$. We use the chain rule to evaluate $\frac{\partial E_{tot}^{Pen}}{\partial u_{\gamma j}^{k}}$

$$\frac{\partial E_{tot}^{Pen}}{\partial u_{\gamma j}^{k}}=\sum_{\alpha\beta}\frac{\partial E_{tot}^{Pen}}{\partial S_{\alpha\beta}}\frac{\partial S_{\alpha\beta}}{\partial u_{\gamma j}^{k}}+\sum_{\alpha\beta}\frac{\partial E_{tot}^{Pen}}{\partial H_{\alpha\beta}}\frac{\partial H_{\alpha\beta}}{\partial u_{\gamma j}^{k}}. \tag{3.7}$$

Observing (3.5), we have

$$\begin{aligned}\frac{\partial E_{tot}^{Pen}}{\partial S_{\alpha\beta}}&=[6(LHL)-4(LSLHL+LHLSL)]_{\beta\alpha}\\&\quad+2\mu[2\mathrm{tr}((3LSL-2LSLSL)S)-N_{el}](6LSL-6LSLSL)_{\beta\alpha},\end{aligned} \tag{3.8a}$$

$$\frac{\partial E_{tot}^{Pen}}{\partial H_{\alpha\beta}}=2(3LSL-2LSLSL)_{\beta\alpha}. \tag{3.8b}$$

Meanwhile, $\frac{\partial S_{\alpha\beta}}{\partial u_{\gamma j}^{k}}$ and $\frac{\partial H_{\alpha\beta}}{\partial u_{\gamma j}^{k}}$ will be given later. When we are minimizing the total energy with respect to $\mathbf{u}$, the object function should be $E_{tot}^{Pen}+E_{tot}^{DG}$. The analytical expressions for the derivatives $\partial E_{tot}^{DG}/\partial u_{\alpha j}^{k}$ is given by

$$\frac{\partial E_{tot}^{DG}}{\partial u_{\alpha j}^{k}}=\frac{a}{h}\int_{\partial I_k}\varphi_k^j(s)(\phi_\alpha(s)|_{I_k}-\phi_\alpha(s)|_{I_k(bd)})ds, \tag{3.9}$$

where $I_k(bd)$ is the neighbor element of I_k, which is next to the certain boundary.

The linear-scaling behavior arises from the spatial localization of the support functions, which implies that the overlap and Hamiltonian matrices $S_{\alpha\beta}$ and $H_{\alpha\beta}$ vanish if the distance between the support functions exceeds a certain cutoff distance. With the cutoff

we are imposing on $L_{\alpha\beta}$, it follows that all matrices appearing in the expressions for E_{tot} and its derivatives are sparse and the number of nonzero elements grows linearly with the number of atoms.

In practice, the minimization is currently performed by making a sequence of conjugate gradients steps for the minimization with respect to the $L_{\alpha\beta}$ coefficients, followed by a sequence of steps for the minimization with respect to the DG coefficients $u_{\alpha k}$ for the support functions, alternating between these two types of iterations.

The above general scheme has been implemented in the local-density approximation (LDA) using the pseudopotential technique and all calculations are done on a grid in real space. In this respect, our techniques have much in common with the real-space grid methods recently developed in [4, 14] for DFT pseudopotential calculations. At the moment, periodic boundary conditions are used to in order to avoid edge effects, but the technique could easily be applied with other boundary conditions.

Though we use discontinuous Galerkin element to approximate support function, the interior penalty term would ensure the support function to be almost continuous when we set the penalty parameter large enough.

4 Algorithm details of the DG-DMM for a 1-D lattice model

In this section, we will apply the DG-DMM method to a one dimensional tight binding model of poly-atomic system [10], whose nuclear potential are represented by a series of Gaussian. Our main objective here in this work is to test the performance of the hybrid enriched basis in the DG approximation and the linear scaling complexity as the number of atoms increases.

Assume that there is an infinite array of atoms on a line with a unit spacing: $X_i = i$, for $i \in \mathbb{Z}$. Each atom has one valence electron and we ignore spin degeneracy. The electrons are noninteracting, so that the electronic structure of the system is determine by solving linear eigenvalue problems (instead of nonlinear eigenvalue problems as in the full Kohn-Sham DFT),

$$\hat{H}\psi_i = \varepsilon_i \psi_i, \tag{4.1}$$

where the Hamiltonian is given by

$$\hat{H} = -\frac{1}{2}\nabla^2 + V(x). \tag{4.2}$$

The effective potential V is a sum of Gaussian wells located at the atom sites

$$V(x) = -\sum_{i\in\mathbb{Z}} \frac{a}{\sqrt{2\pi\sigma^2}} \exp\left[-(x-X_i)^2/2\sigma^2\right]. \tag{4.3}$$

This model has two parameters: a, which characterizes the depth of the wells, and σ, which characterizes its width.

The parameters of the problem are as follows:

- N — number of atoms;
- periodic boundary condition;
- $\phi_{i\alpha}$, i indicates the atoms, α the orbitals on each atom, and $\phi_{i,\alpha}$ is the basis orbitals at atom i;
- $H_{i\alpha,j\beta}=<i\alpha|\hat{H}|j\beta>$;
- Find the minimum of the total energy $E_{tot}=2\mathrm{tr}(\hat{\rho}\hat{H})$ under constraints: (1) fixed number of electrons, (2) idempotency, i.e., $\hat{\rho}^2=\hat{\rho}$.

In the first subsection, we discuss the formulae about the auxiliary function σ. In the next two subsections, we discuss the derivation of formulae about the overlap matrix and Hamiltonian matrix without the terms of local orbital function. In the fourth section, we add the terms of local orbital function and obtain the final formulae.

4.1 Auxiliary variable $\sigma(x)=\phi'(x)$

In order to achieve the connection between the DG basis functions in neighboring elements, we introduce an auxiliary function(s) to approximate the gradient of the support function $\phi(\mathbf{r})$ (the index of support function is omitted)

$$\sigma(\mathbf{r})=\nabla\phi(\mathbf{r}), \tag{4.4}$$

which is assumed to have a corresponding representation as

$$\sigma(\mathbf{r})=\nabla u^{lo}(\mathbf{r})+\sum_{k,j}\sigma_j^k\varphi_k^j(\mathbf{r}), \tag{4.5}$$

where $\nabla u^{lo}(\mathbf{r})$ is also localized by truncations. Plugging (3.1) and (4.5) into (4.4), we have

$$\sum_{k,j}\sigma_j^k\varphi_j^k(\mathbf{r})=\nabla u(\mathbf{r})=\nabla\sum_{k,j}u_j^k\varphi_j^k(\mathbf{r}). \tag{4.6}$$

In the finite element method, a weak form of (4.6) is used instead, which is obtained by multiplying its both sides by a test function $\varphi_i^l(\mathbf{r})$, and using integration by parts,

$$\begin{aligned}\sum_{k,j}\sigma_j^k\int_{I_l}\varphi_j^k(\mathbf{r})\varphi_i^l(\mathbf{r})d\mathbf{r}&=\int_{I_l}\nabla u(\mathbf{r})\varphi_i^l(\mathbf{r})d\mathbf{r}\\&=\int_{\partial I_l}u(\mathbf{r})\varphi_i^l(\mathbf{r})\mathbf{n}d\mathbf{s}-\int_{I_l}u(\mathbf{r})\nabla\varphi_i^l(\mathbf{r})d\mathbf{r},\end{aligned} \tag{4.7}$$

where $\mathbf{n}$ is the norm unit outward vector to the boundary ∂I_l. However, the support function $u(\mathbf{r})$ has two values — indicated by $+$ and $-$, on the boundary ∂I_l due to the discontinuous representation in (3.1). To remove this ambiguity, a unique quantity — numerical flux $h(u^-,u^+)$, will be defined on the boundary to approximate the true flux

$f(u)$. There are various constructions of the numerical fluxes such as taking the average of the $u^{\pm}$ (central flux) or the value on one side (upwinding). The numerical flux is required to satisfy a consistent condition, namely, if u has no discontinuity at the common interface of two elements, then we should have

$$h(u^-,u^+)=f(u), \quad \text{if} \quad u^-=u^+=u. \tag{4.8}$$

In this paper, we will use the upwinding approach as it results in a more compact representation of the Hamiltonian. Replacing the term on the element boundary in (4.7) by the numerical flux, we have for each basis function φ_i^l on element I_l

$$\sum_{k,j}\sigma_j^k\int_{I_l}\varphi_j^k(\mathbf{r})\varphi_i^l(\mathbf{r})dr=\int_{\partial I_l}h(u^-,u^+)\varphi_i^l(\mathbf{r})\mathbf{n}d\mathbf{s}-\int_{I_l}u(\mathbf{r})\nabla\varphi_i^l(\mathbf{r})d\mathbf{r}, \tag{4.9}$$

which gives a linear system for the coefficients $\boldsymbol{\sigma}^k$ on each of the element I_l,

$$S^l\boldsymbol{\sigma}^k=\mathbf{b}, \tag{4.10}$$

where the local mass matrix $(S^l)_{ij}=\int_{I_l}\varphi_i^l(\mathbf{r})\varphi_j^l(\mathbf{r})d\mathbf{r}$, the right hand side $\mathbf{b}$ depending on $u^{l'}$, $I_{l'}\cap I_l\neq\varnothing$. We can express the coefficients $\boldsymbol{\sigma}^k$ in terms of coefficient $u^{l'}$ from the neighboring elements $I_{l'}$,

$$\boldsymbol{\sigma}^k=(S^l)^{-1}\mathbf{b}. \tag{4.11}$$

We will provide the explicit formula of $\boldsymbol{\sigma}^k$, which allows explicit formulae for the differentiation $\frac{\partial\sigma_i^k}{\partial u_j^l}$. Rewriting Eq. (4.9) for each element I_k without the term of local orbital function, in 1-D case we have

$$\sum_j S_{ij}^k\sigma_j^k=\varphi_i^k(x)h_\phi(x)\Big|_{x_{k-1/2}}^{x_{k+1/2}}-\int_{I_k}\phi(x)\frac{d}{dx}\varphi_i^k(x)dx, \tag{4.12}$$

with an upwinding flux,

$$h_\phi(x_{k+1/2})=\phi(x_{k+1/2}^-), \tag{4.13}$$

we have

$$\sum_l S_{ij}^k\sigma_j^k=\varphi_i^k(x_{k+1/2})\phi(x_{k+1/2}^-)-\varphi_i^k(x_{k-1/2})\phi(x_{k-1/2}^-)-\sum_j M_{ij}^k u_j^k, \tag{4.14}$$

where the local overlap matrix

$$S_{ij}^k=\int_{I_k}\varphi_i^k(x)\varphi_j^k(x)dx, \tag{4.15}$$

and

$$S^k=\{S_{ij}^k\}. \tag{4.16}$$

For the local stiffness matrix,

$$M_{ij}^k = \int_{I_k} \varphi_j^k(x) \frac{d}{dx} \varphi_i^k(x) dx, \tag{4.17}$$

and

$$M^k = \{M_{ij}^k\}. \tag{4.18}$$

After introducing the following notations:

$$\mathbf{u}^k = (u_0^k, \cdots, u_j^k, \cdots)^T, \tag{4.19a}$$

$$\boldsymbol{\sigma}^k = (\sigma_0^k, \cdots, \sigma_j^k, \cdots)^T, \tag{4.19b}$$

$$\boldsymbol{\varphi}^k(x_{k+1/2}) = (\varphi_0^k(x_{k+1/2}), \cdots, \varphi_j^k(x_{k+1/2}), \cdots)^T, \tag{4.19c}$$

$$(\mathbf{u}^k, \boldsymbol{\varphi}^k(x_{k+1/2})) = (\mathbf{u}^k)^T \boldsymbol{\varphi}^k(x_{k+1/2}) = \sum_j u_j^k \varphi_j^k(x_{k+1/2}), \tag{4.19d}$$

we can rewrite (4.14) as

$$\begin{aligned} S^k \boldsymbol{\sigma}^k =& \boldsymbol{\varphi}^k(x_{k+1/2})(\boldsymbol{\varphi}^k(x_{k+1/2}))^T \mathbf{u}^k \\ & - \boldsymbol{\varphi}^k(x_{k-1/2})(\boldsymbol{\varphi}^{k-1}(x_{k-1/2}))^T \mathbf{u}^{k-1} - M^k \mathbf{u}^k, \end{aligned} \tag{4.20}$$

or equivalently

$$\begin{aligned} \boldsymbol{\sigma}^k =& (S^k)^{-1} \Big[\boldsymbol{\varphi}^k(x_{k+1/2})(\boldsymbol{\varphi}^k(x_{k+1/2}))^T \mathbf{u}^k \\ & - \boldsymbol{\varphi}^k(x_{k-1/2})(\boldsymbol{\varphi}^{k-1}(x_{k-1/2}))^T \mathbf{u}^{k-1} - M^k \mathbf{u}^k \Big]. \end{aligned} \tag{4.21}$$

From (4.21), we obtain the derivative of the i-th component of the coefficient σ^k with respect to the j-th component of the coefficient u^l,

$$\begin{aligned} \frac{\partial \sigma_i^k}{\partial u_j^l} =& \delta_{kl} \left\{ (S^k)^{-1} \left[\boldsymbol{\varphi}^k(x_{k+1/2}) \left(\boldsymbol{\varphi}'^k(x_{k+1/2}) \right)^T - M^k \right] \right\}_{ij} \\ & - \delta_{(k-1)l} \left\{ (S^k)^{-1} \left[\boldsymbol{\varphi}^k(x_{k-1/2}) \left(\boldsymbol{\varphi}^{k-1}(x_{k-1/2}) \right)^T \right] \right\}_{ij}. \end{aligned} \tag{4.22}$$

We will also use the notation:

$$\tilde{M}^{k,l} = \left\{ \frac{\partial \sigma_i^k}{\partial u_j^l} \right\}. \tag{4.23}$$

In a traditional DG implementation without using local orbital function in (3.1), the support function $\phi(x)$ is expressed into the linear combination of the DG piecewise polynomial basis functions $\varphi_j^k(x)$,

$$\phi(x) = \sum_{k,j} u_j^k \varphi_j^k(x), \tag{4.24}$$

where the index k is for the element I_k and j is the index of the DG basis function on the element I_k. The number of DG basis functions on different element I_k can be different. $\varphi_j^k(x)$ can be chosen to be the Legendre polynomial of order j on the element I_k and to be zero on the other elements.

4.2 Calculation of the overlap matrix $S_{\alpha\beta}$

The global overlap matrix can be expressed in terms of the local overlap matrices in (4.16),

$$S_{\alpha\beta}=\int_\Omega \phi_\alpha(x)\phi_\beta(x)dx=\sum_k\int_{I_k}\phi_\alpha(x)\phi_\beta(x)dx=\sum_k S^k_{\alpha\beta}. \tag{4.25}$$

From the above equation, we can calculate the derivative of $S_{\alpha\beta}$ with respect to $u^l_{\gamma i}$ with the formula

$$\frac{\partial S_{\alpha\beta}}{\partial u^l_{\gamma i}}=\sum_k\frac{\partial S^k_{\alpha\beta}}{\partial u^l_{\gamma i}}, \tag{4.26a}$$

$$\frac{\partial S^k_{\alpha\beta}}{\partial u^l_{\gamma i}}=\delta_{kl}\left[\delta_{\alpha\gamma}S^k u^k_\beta+\delta_{\beta\gamma}S^k u^k_\alpha\right]_i. \tag{4.26b}$$

4.3 Hamiltonian matrix $H_{\beta\alpha}=\int_\Omega \phi_\alpha(x)\hat{H}\phi_\beta(x)dx$

In the following, we use the Hartree atom units for simplicity, i.e., the numerical values of the following four fundamental physical constants:

- electron mass m,
- elementary charge q_e,
- reduced Planck's constant $\hbar$,
- Coulomb's const $\frac{1}{4\pi\epsilon_0}$.

The total energy will be expressed into

$$E_{tot}=2\sum_{\alpha,\beta}K_{\alpha\beta}H_{\beta\alpha}. \tag{4.27}$$

For the Hamiltonian operator given in (4.2), we have

$$H_{\beta\alpha}=H^{\text{kinetic}}+H^{\text{pot}}, \tag{4.28}$$

where the kinetic energy

$$H^{\text{kinetic}}_{\beta\alpha}=-\frac{1}{2}\int_\Omega \phi_\alpha(x)\frac{d^2}{dx^2}\phi_\beta(x)dx, \tag{4.29}$$

and the potential energy

$$H_{\beta\alpha}^{\text{pot}}=\int_{\Omega}V(x)\phi_{\alpha}(x)\phi_{\beta}(x)dx. \tag{4.30}$$

If $V(x)=V^k$ is a constant in the element I_k, we can obtain $H_{\beta\alpha}^{\text{pot}}$ and $\frac{\partial H_{\beta\alpha}^{\text{pot}}}{\partial u_{\gamma,i}^l}$ as what we have done in (4.25) and (4.26a). Generally, we have

$$H_{\beta\alpha}^{\text{pot}}=\int_{\Omega}\phi_{\alpha}(x)V(x)\phi_{\beta}(x)dx=\sum_k H_{\beta\alpha}^{\text{pot},k}, \tag{4.31}$$

where

$$H_{\beta\alpha}^{\text{pot},k}=\int_{I_k}\phi_{\alpha}(x)V(x)\phi_{\beta}(x)dxdx=\left(u_{\alpha}^k\right)^T S^{\text{pot},k}u_{\beta}^k, \tag{4.32}$$

and

$$S_{ij}^{\text{pot},k}=\int_{I_k}\varphi_i^k(x)V(x)\varphi_j^k(x)dx. \tag{4.33}$$

From the above equation, we can calculate the derivative of $H_{\beta\alpha}^{\text{pot}}$ with respect to $u_{\gamma i}^l$ as follows,

$$\frac{\partial H_{\beta\alpha}^{\text{pot}}}{\partial u_{\gamma i}^l}=\sum_k\frac{\partial H_{\beta\alpha}^{\text{pot},k}}{\partial u_{\gamma i}^l}, \tag{4.34a}$$

$$\frac{\partial H_{\beta\alpha}^{\text{pot},k}}{\partial u_{\gamma i}^l}=\delta_{kl}\left[\delta_{\alpha\gamma}S^{\text{pot},k}u_{\beta}^k+\delta_{\beta\gamma}S^{\text{pot},k}u_{\alpha}^k\right]_i. \tag{4.34b}$$

Next, for the kinetic energy term, we first rewrite (4.29) as

$$H_{\beta\alpha}^{\text{kinetic}}=-\frac{1}{2}\int_{\Omega}\phi_{\alpha}(x)\nabla\sigma_{\beta}(x)dx, \tag{4.35}$$

and express $\phi_{\alpha}(x)$ and $\phi_{\beta}(x)$ with the linear combination of the DG basis functions

$$\phi_{\alpha}(x)=\sum_{k,j}u_{\alpha,j}^k\varphi_j^k(x),\qquad \phi_{\beta}(x)=\sum_{k,j}u_{\beta,j}^k\varphi_j^k(x), \tag{4.36}$$

and, similarly, $\sigma_{\alpha}(x)$ and $\sigma_{\beta}(x)$

$$\sigma_{\alpha}(x)=\sum_{k,j}\sigma_{\alpha,j}^k\varphi_l^k(x),\qquad \sigma_{\beta}(x)=\sum_{k,j}\sigma_{\beta,j}^k\varphi_j^k(x). \tag{4.37}$$

And (4.35) will be calculated by integration by parts and introducing appropriate numerical fluxes for $\sigma_{\beta}(x)$ at the boundary of each element I_k, namely,

$$H_{\beta\alpha}^{\text{kinetic}}=\sum_k H_{\beta\alpha}^{\text{kinetic},k}, \tag{4.38}$$

where

$$H_{\beta\alpha}^{\text{kinetic},k} = -\frac{1}{2}\int_{I_k} \phi_\alpha(x)\nabla\sigma_\beta(x)dx$$
$$= -\frac{1}{2}\left[\int_{\partial I_k} \phi_\alpha(x)h_\sigma(\sigma_\beta(x^-),\sigma_\beta(x^+))ds - \int_{I_k}\left(\frac{d}{dx}\phi_\alpha(x)\right)\sigma_\beta(x)dx\right]. \tag{4.39}$$

In 1-D case, the boundary flux in (4.39) would be written as

$$h_\sigma\left(\sigma_\beta(x_{k+1/2}^-),\sigma_\beta(x_{k+1/2}^+)\right) = \sigma_\beta(x_{k+1/2}^+), \tag{4.40}$$

which is similar to (4.13) but is on an opposite side. Replacing $\frac{d}{dx}\phi_\alpha(x)$ in (4.39) with $\sigma_\alpha(x)$, we have

$$H_{\beta\alpha}^{\text{kinetic},k} = -\frac{1}{2}\int_{I_k} \phi_\alpha(x)\frac{d}{dx}\sigma_\beta(x)dx$$
$$= -\frac{1}{2}\Big[(u_\alpha^k,\varphi^k(x_{k+1/2}))(\sigma_\beta^{k+1},\varphi^{k+1}(x_{k+1/2}))$$
$$-(u_\alpha^k,\varphi^k(x_{k-1/2}))(\sigma_\beta^k,\varphi^k(x_{k-1/2})) - \int_{I_k}\sigma_\alpha(x)\sigma_\beta(x)dx\Big], \tag{4.41}$$

or in a matrix-vector product form

$$H_{\beta\alpha}^{\text{kinetic},k} = -\frac{1}{2}\Big[\left(u_\alpha^k\right)^T\varphi^k(x_{k+1/2})\left(\varphi^{k+1}(x_{k+1/2})\right)^T\sigma_\beta^{k+1}$$
$$-\left(u_\alpha^k\right)^T\varphi^k(x_{k-1/2})\left(\varphi^k(x_{k-1/2})\right)^T\sigma_\beta^k - \left(\sigma_\alpha^k\right)^T S^k\sigma_\beta^k\Big]. \tag{4.42}$$

Using the matrix-form of the $H_{\beta\alpha}^{\text{kinetic},k}$ (4.42), and the derivative $\frac{\partial u'^k_i}{\partial u^l_j}$ (4.21), we obtain

$$\frac{\partial H_{\beta\alpha}^{\text{kinetic}}}{\partial u_{\gamma,j}^l} = \sum_k \frac{\partial H_{\beta\alpha}^{\text{kinetic},k}}{\partial u_{\gamma,j}^l}, \tag{4.43}$$

where

$$\frac{\partial H_{\beta\alpha}^{\text{kinetic},k}}{\partial u_{\gamma,j}^l} = \Big[\delta_{kl}\delta_{\alpha\gamma}\left(\sigma_\beta^{k+1}\right)^T\varphi^{k+1}(x_{k+1/2})\varphi^k(x_{k+1/2})$$
$$+\left(u_\alpha^k\right)^T\varphi^k(x_{k+1/2})\delta_{\beta\gamma}\left(\tilde{M}^{k+1,l}\right)^T\varphi^{k+1}(x_{k+1/2})$$
$$-\delta_{kl}\delta_{\alpha\gamma}\left(\sigma_\beta^k\right)^T\varphi^k(x_{k-1/2})\varphi^k(x_{k-1/2})$$
$$-\left(u_\alpha^k\right)^T\varphi^k(x_{k-1/2})\delta_{\beta\gamma}\left(\tilde{M}^{k,l}\right)^T\varphi^k(x_{k-1/2})$$
$$-\delta_{\alpha\gamma}\left(\tilde{M}^{k,l}\right)^T S^k\sigma_\beta^k - \delta_{\beta\gamma}\left(\tilde{M}^{k,l}\right)^T S^k\sigma_\alpha^k\Big]_j. \tag{4.44}$$

Finally, from (4.28), (4.31) and (4.43), we can obtain $\frac{\partial H_{\beta\alpha}}{\partial u^l_{\gamma i}}$.

4.4 Physics-based local orbitals enriched DG approximation of $\phi_\alpha(x)$

In this case, we have the support functions and their derivatives approximated by

$$\phi(x) = u^{lo}(x) + u^d(x), \tag{4.45a}$$

$$\sigma(x) = \nabla u^{lo}(x) + \sigma^d(x), \tag{4.45b}$$

where $u^d(x)$ and $\sigma^d(x)$ are the same as the second term in (3.1) and (4.5), and their coefficients are related by (4.21). We use the local orbital function $u^{lo}(x)$ and its derivative $\nabla u^{lo}(x)$ are localized by truncations.

Next we exam what happens to the overlap matrix S and the Hamiltonian matrix H when local orbital functions $u^{lo}(x)$ are included in the representation of the support function $\phi_\alpha(x)$. In this case, we have the overlap matrix

$$\begin{aligned} S_{\alpha\beta} &= \int_\Omega \phi_\alpha(x)\phi_\beta(x)dx \\ &= \int_\Omega [u^d_\alpha(x) + u^{lo}_\alpha(x)][u^d_\beta(x) + u^{lo}_\beta(x)]dx \\ &= \int_\Omega u^d_\alpha(x)u^d_\beta(x)dx + \int_\Omega u^{lo}_\alpha(x)u^d_\beta(x)dx \\ &\quad + \int_\Omega u^d_\alpha(x)u^{lo}_\beta(x)dx + \int_\Omega u^{lo}_\alpha(x)u^{lo}_\beta(x)dx. \end{aligned} \tag{4.46}$$

First, we will show the matrix form of $S_{\alpha\beta}$ and its derivative with respect to $u^l_{\gamma i}$. We rewrite $S_{\alpha\beta}$ of (4.46) in four terms:

$$S_{\alpha\beta} = \sum_k S^k_{\alpha\beta} = \sum_k (S^{k1}_{\alpha\beta} + S^{k2}_{\alpha\beta} + S^{k3}_{\alpha\beta} + S^{k4}_{\alpha\beta}), \tag{4.47}$$

where

$$S^{k1}_{\alpha\beta} = \int_{I_k} u^d_\alpha(x)u^d_\beta(x)dx, \qquad S^{k2}_{\alpha\beta} = \int_{I_k} u^{lo}_\alpha(x)u^d_\beta(x)dx, \tag{4.48a}$$

$$S^{k3}_{\alpha\beta} = \int_{I_k} u^d_\alpha(x)u^{lo}_\beta(x)dx, \qquad S^{k4}_{\alpha\beta} = \int_{I_k} u^{lo}_\alpha(x)u^{lo}_\beta(x)dx. \tag{4.48b}$$

The derivative of the first term $S^{k1}_{\alpha\beta}$ was shown in Section 4.2. The second term becomes

$$\begin{aligned} S^{k2}_{\alpha\beta} &= \int_{I_k} u^{lo}_\alpha(x) \sum_j u^k_{\beta j}\varphi^k_j(x)dx \\ &= \sum_j \left(\int_{I_k} u^{lo}_\alpha(x)\varphi^k_j(x)dx \right) \times u^k_{\beta j}. \end{aligned} \tag{4.49}$$

The derivative of $S^{k2}_{\alpha\beta}$ is

$$\frac{\partial S^{k2}_{\alpha\beta}}{\partial u^l_{\gamma i}} = \delta_{kl}\delta_{\beta\gamma}\Gamma^k_{\alpha i}, \tag{4.50}$$

where $\Gamma^k_{\alpha i} = \int_{I_k} u^{lo}_\alpha \varphi^k_i dx$. The derivative of the third term can be written in the same way. Thus the derivative of $S^k_{\alpha\beta}$ is

$$\frac{\partial S^k_{\alpha\beta}}{\partial u^l_{\gamma i}} = \delta_{kl}\left[\delta_{\alpha\gamma}S^k u^k_\beta + \delta_{\beta\gamma}S^k u^k_\alpha\right]_i + \delta_{kl}\left(\delta_{\beta\gamma}\Gamma^k_{\alpha i} + \delta_{\alpha\gamma}\Gamma^k_{\beta i}\right). \tag{4.51}$$

In 1-D case, for the Hamiltonian matrix, we have

$$\begin{aligned} H^{\text{kinetic}}_{\beta\alpha} &= \int_\Omega \left[u^d_\alpha(x) + u^{lo}_\alpha(x)\right]\frac{d}{dx}\left[\sigma^d_\beta(x) + u^{lo\prime}_\beta(x)\right]dx \\ &= \int_\Omega u^d_\alpha(x)\frac{d}{dx}\sigma^d_\beta(x)dx + \int_\Omega u^{lo}_\alpha(x)\frac{d}{dx}\sigma^d_\beta(x)dx \\ &\quad + \int_\Omega u^d_\alpha(x)\frac{d}{dx}u^{lo\prime}_\beta(x)dx + \int_\Omega u^{lo}_\alpha(x)\frac{d}{dx}u^{lo\prime}_\beta(x)dx. \end{aligned} \tag{4.52}$$

where the $'$ denotes differentiation. The calculation of $\int_\Omega u^d_\alpha(x)\frac{d}{dx}\sigma^d_\beta(x)dx$ in (4.52) has been discussed and given in the previous section. The second term in (4.52) is

$$\int_\Omega u^{lo}_\alpha(x)\frac{d}{dx}\sigma^d_\beta(x)dx = \sum_k \int_{I_k} u^{lo}_\alpha(x)\frac{d}{dx}\sigma^d_\beta(x)dx, \tag{4.53}$$

where

$$\begin{aligned} \int_{I_k} u^{lo}_\alpha(x)\frac{d}{dx}\sigma^d_\beta(x)dx &= u^{lo}_\alpha(x_{k+1/2})\sigma^d_\beta(x^+_{k+1/2}) \\ &\quad - u^{lo}_\alpha(x_{k-1/2})\sigma^d_\beta(x^+_{k-1/2}) - \int_{I_k} u^{lo\prime}_\alpha(x)\sigma^d_\beta(x)dx. \end{aligned} \tag{4.54}$$

Using the fact that $u^{lo}_\alpha(x)$ and $\sigma^d_\beta(x)$ are periodic, we have

$$\int_\Omega u^{lo}_\alpha(x)\frac{d}{dx}\sigma^d_\beta(x)dx = -\sum_k \int_{I_k} u^{lo\prime}_\alpha(x)\sigma^d_\beta(x)dx. \tag{4.55}$$

The third term in (4.52) reads

$$\int_\Omega u^d_\alpha(x)\frac{d}{dx}u^{lo\prime}_\beta(x)dx = \sum_k \int_{I_k} u^d_\alpha(x)\frac{d}{dx}u^{lo\prime}_\beta(x)dx, \tag{4.56}$$

where

$$\int_{I_k} u_\alpha^d(x)\frac{d}{dx}u_\beta^{lo\prime}(x)dx = u_\alpha^d(x_{k+1/2}^-)u_\beta^{lo\prime}(x_{k+1/2}) - u_\alpha^d(x_{k-1/2}^+)u_\beta^{lo\prime}(x_{k-1/2}) - \int_{I_k}\sigma_\alpha^d(x)u_\beta^{lo\prime}(x)dx. \tag{4.57}$$

The fourth term in (4.52) becomes

$$\int_\Omega u_\alpha^{lo}(x)\frac{d}{dx}u_\beta^{lo\prime}(x)dx = u_\alpha^{lo}(x)u_\beta^{lo\prime}(x)\Big|_{\partial\Omega} - \int_\Omega u_\alpha^{lo\prime}(x)u_\beta^{lo\prime}(x)dx. \tag{4.58}$$

Using the fact that $u^{lo}(x)$ and $u^{lo\prime}(x)$ are periodic, we can reduce (4.58) into

$$\int_\Omega u_\alpha^{lo}(x)\frac{d}{dx}u_\beta^{lo\prime}(x)dx = -\int_\Omega u_\alpha^{lo\prime}(x)u_\beta^{lo\prime}(x)dx. \tag{4.59}$$

Now, we can find the derivative of $H_{\alpha\beta}^{kinect}$ with respect to $u_{\gamma i}^l$. For the purpose, we denote

$$H_{\alpha\beta}^{\text{kinetic}} = \sum_k H_{\alpha\beta}^{\text{kinetic,k}} = \sum_k (H_{\alpha\beta}^{\text{kinetic,k1}} + H_{\alpha\beta}^{\text{kinetic,k2}} + H_{\alpha\beta}^{\text{kinetic,k3}} + H_{\alpha\beta}^{\text{kinetic,k4}}). \tag{4.60}$$

The derivative of first term is calculated in Section 4.3. According to (4.55), the derivative of the second term is

$$\frac{\partial H_{\alpha\beta}^{\text{kinectic},k2}}{\partial u_{\gamma i}^l} = -\delta_{\beta\gamma}\left((\tilde{M}^{k,l})^T\tilde{\Gamma}_\alpha^k\right)_i, \tag{4.61}$$

where

$$\tilde{\Gamma}_\alpha^k = \left(\int_{I_k} u_\alpha^{lo\prime}\varphi_0^k dx, \cdots, \int_{I_k} u_\alpha^{lo\prime}\varphi_i^k dx, \cdots\right)^T. \tag{4.62}$$

According to (4.57), the derivative of the third term is

$$\frac{\partial H_{\alpha\beta}^{\text{kinectic},k3}}{\partial u_{\gamma i}^l} = \delta_{kl}\delta_{\alpha\gamma}\left(u_\beta^{lo\prime}(x_{k+1/2})\varphi^k(x_{k+1/2}) - u_\beta^{lo\prime}(x_{k-1/2})\varphi^k(x_{k-1/2})\right)_i - \delta_{\alpha\gamma}((\tilde{M}^{k,l})^T\tilde{\Gamma}_\beta^k)_i. \tag{4.63}$$

Thus, the derivative of $H_{\alpha\beta}^{\text{kinectic}}$ can be written as combination of (4.44), (4.61) and (4.63). In addition, the derivative of $H_{\alpha\beta}^{\text{pot}}$ can be calculated the same way as the derivative of $S_{\alpha\beta}$.

4.5 Choose local orbitals

We set a single atom Hamiltonian for the atom at position 0

$$\hat{H}_{\text{atom}} = -\frac{1}{2}\frac{d^2}{dx^2} + V_{\text{atom}}(x), \tag{4.64}$$

where

$$V_{\text{atom}}(x) = \frac{a}{\sqrt{2\pi\sigma^2}} \exp\left(-\frac{x^2}{2\sigma^2}\right). \tag{4.65}$$

We can use a finite difference method to solve the eigen problem

$$\hat{H}_{\text{atom}}\psi_i(x) = \varepsilon_i \psi_i(x). \tag{4.66}$$

After we get the eigen-solutions, the local orbitals can be found by a fitting procedure using the Levenberg-Marquardt method as

$$\psi_i(x) \approx P_i(x) \exp\left(-\left(\frac{x}{G}\right)^2\right), \tag{4.67}$$

where $P_i(x)$ is a polynomial function of i-th order. For example,

$$\psi_0(x) \approx B \exp\left(-\left(\frac{x}{G}\right)^2\right). \tag{4.68}$$

Also we will modify the local orbitals obtained into a periodic function on the inter $[0,L]$ (where $L = N_{\text{atom}}$) where the atom is at the position R_{atom}. In one period $x \in [0,L]$, we define

$$\psi_0(x;R_{\text{atom}}) = \begin{cases} B\exp\left(-\left(\frac{x-R_{\text{atom}}}{G}\right)^2\right), & \text{if } |x-R_{\text{atom}}| < \frac{N_{\text{atom}}}{2}, \\ B\exp\left(-\left(\frac{x+N_{\text{atom}}-R_{\text{atom}}}{G}\right)^2\right), & \text{if } x-R_{\text{atom}} < -\frac{N_{\text{atom}}}{2}, \\ B\exp\left(-\left(\frac{x-N_{\text{atom}}-R_{\text{atom}}}{G}\right)^2\right), & \text{if } x-R_{\text{atom}} > \frac{N_{\text{atom}}}{2}. \end{cases} \tag{4.69}$$

5 Numerical tests

5.1 Convergence

The calculation domain contains 8 atoms which locate at 0,1,2,$\cdots$,7, respectively. The periodic boundary condition is used. In this subsection, we will study two systems which model insulator and semiconductor, respectively.

5.1.1 Insulator case

We study the case for which the system models an insulator [10], i.e., a=1000 and σ=0.15.

First, we use central difference to discretize and use the diagonalization method to get the reference ground state energy. Then we present the ground state energy and the error with respect to the reference energy of two methods, LODG (local orbital enriched DG) and DG only, by h-refinement in Fig. 1. We use quadratic polynomial as basis functions in DG part. The Δx stands for the mesh size. Obviously, the ground state energy from the calculation decreases monotonically towards the reference energy when we refine the mesh size. We also present the result by p-refinement in Fig. 2 with the mesh size $\Delta x = \frac{1}{40}$. We can conclude that when we raise the degree of basis polynomial functions in each element, the ground state energy decreases towards the reference energy. The

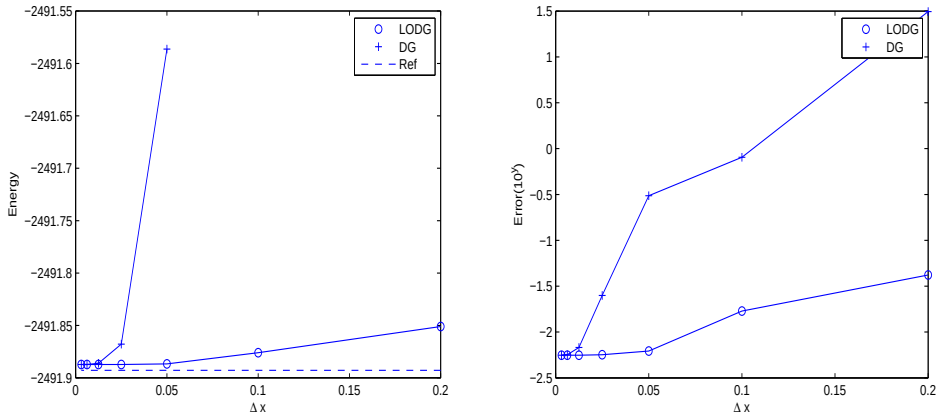

Figure 1: Left: ground state energy with different mesh size by LODG and pure DG only. Right: error of ground state energy with different mesh size by LODG and pure DG only.

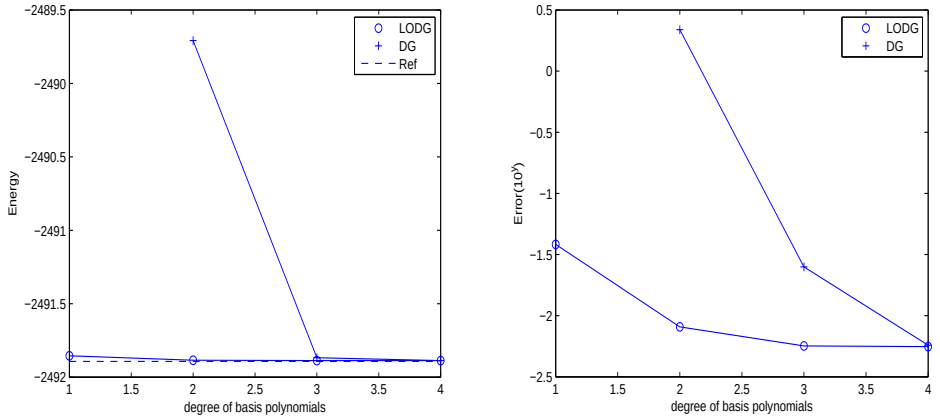

Figure 2: Left: ground state energy with different degree of basis polynomials by LODG and pure DG only. Right: error of ground state energy with different degree of basis polynomials by LODG and pure DG only.

reasons that the error converges at about 10^{-2} are two-fold. The first is that the reference ground state energy is calculated numerically. The second one is that there is a system error between the minimizations by the wave function method and by the density matrix method.

Comparing the results from two methods, LODG and pure DG only, in Figs. 1 and 2, LODG shows its advantage when we use coarse mesh or low degree basis functions. That means we can get a fine result with less calculation by using LODG. Meanwhile, when the mesh size was refined or the degree of basis polynomial was raised, pure DG only method performs as well as LODG.

5.1.2 Semiconductor

We study the case for which the system models a semiconductor [10], i.e., $a=10$ and $\sigma=0.3$.

We use central difference to discretize and use the diagonalization method to get the reference ground state energy. We present the error of ground state energy with respect to the reference energy of two methods, LODG (local orbital enriched DG) and DG only, by h-refinement and p-refinement in Fig. 3. In h-refinement case, we use quadratic polynomial as basis functions in DG part. The Δx stands for the mesh size. The ground state energy from the calculation converges towards the reference energy when we refine the mesh size. In p-refinement, we use mesh size $\Delta x=\frac{1}{40}$. We can conclude that when we raise the degree of basis polynomial functions in each element, the ground state energy converges towards the reference energy.

Comparing the results from two methods, LODG and pure DG only, in Fig. 3, LODG shows its advantage when we use coarse mesh or low degree basis functions. That means we can get a fine result with less calculation by using LODG. Meanwhile, when the mesh size was refined or the degree of basis polynomial was raised, DG only method performs as well as LODG.

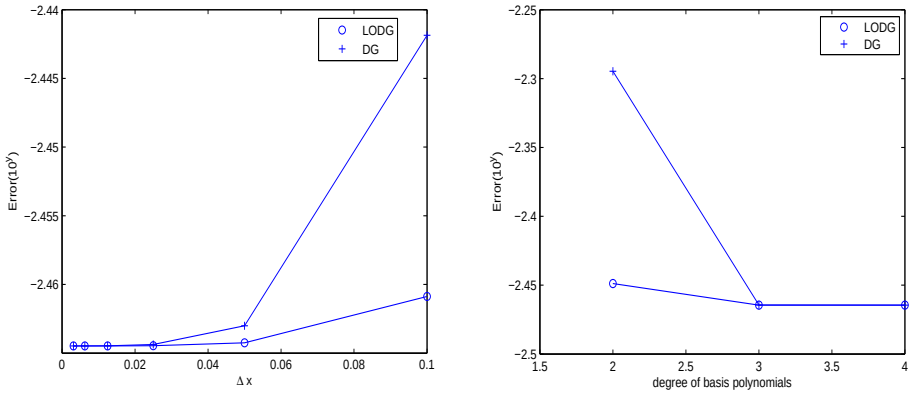

Figure 3: Left: error of total energy with different mesh size by LODG and DG only in h-refinement. Right: error of total energy with different degree of basis polynomials by LODG and DG only in p-refinement.

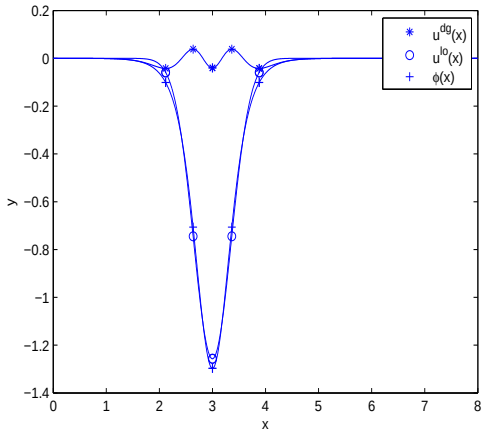

Figure 4: Support function ϕ and its two parts, local orbital part u^{lo} and DG part u^{dg}.

We draw a support function, $\phi_4 = u^{lo} + u^{dg}$, in Fig. 4. We can observe that the local orbital part domain the main part of the support function while the DG part provide small correction.

5.2 Nonlinear system

The Hamiltonian of the previous test is given by

$$\hat{H} = -\frac{1}{2}\frac{d^2}{dx^2} + V(x), \tag{5.1}$$

where the potential

$$V(x) = V_{\mathbf{ps}} = -\sum_i \frac{a}{\sqrt{2\pi\sigma^2}} \exp\left[-(x - X_i)^2/2\sigma^2\right] \tag{5.2}$$

is given and the $\hat{H}$ is a linear operator.

Now, we introduce the exchange potential and Hartree potential

$$V(x) = V_{\mathbf{ps}} + V_{\mathbf{ex}} + V_H. \tag{5.3}$$

We can use local density approximation to calculate exchange potential term [15] as

$$V_{\mathbf{ps}}(r) = -\frac{1}{\pi}(3\pi^2\rho(r,r))^{\frac{1}{3}}. \tag{5.4}$$

We can get the Hartree potential by solving Poisson equation

$$\nabla^2 V_H(r) = -4\pi\rho(r,r). \tag{5.5}$$

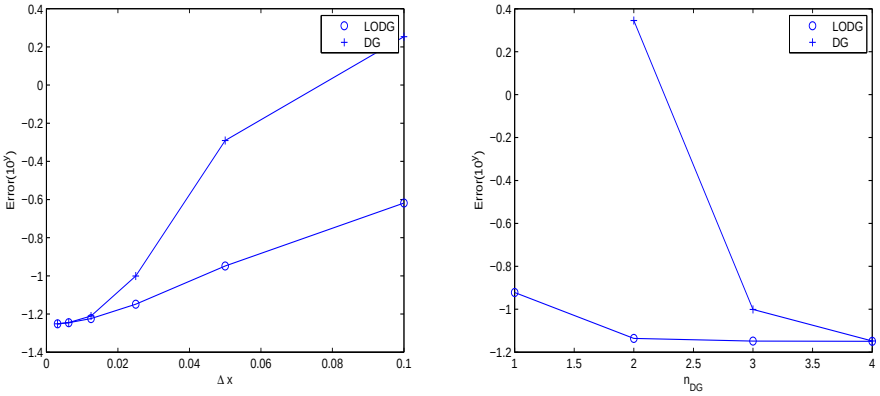

Figure 5: Left: error of ground state energy with different mesh size by LODG and pure DG in h-refinement. Right: error of ground state energy with different degree of basis polynomials by LODG and pure DG only in p-refinement.

We use self-consistent iteration to solve the nonlinear system. As in former cases, we use central difference to discretize $\hat{H}$ and use the diagonalization method to get the reference ground state energy. We present the error of ground state energy with respect to the reference energy of two methods, LODG(local orbital enriched DG) and DG only, by h-refinement and p-refinement in Fig. 5. In h-refinement case, we use quadratic polynomial as basis functions in DG part. In p-refinement, we use mesh size $\Delta x = \frac{1}{40}$. We can observe that the ground state energy also decrease towards the reference energy but the accuracy is not as good as the linear case due to error in the self-consistent iteration.

5.3 Linear scaling performance

The degree of matrices H, S, L is the number of support function, which is $\nu N = O(N)$. Considering the cut-off radius, if $|X_\alpha - X_\beta| > 2R_{reg}$ then $H_{\alpha\beta}$,$S_{\alpha\beta}$,$L_{\alpha\beta}$ equal zero. Thus, matrices H,S,L are sparse and the numbers of non-zero terms are $\mathcal{O}(N)$. The calculation of $H_{\alpha\beta}$,$S_{\alpha\beta}$,$L_{\alpha\beta}$ only involve the multiplication of matrices of which the degree is the number of basis function in each element, which can be considered as $\mathcal{O}(1)$. We can conclude that the calculation time is linear scaling with N (the number of atoms).

We studied the linear system which models an insulator using LODG with quadratic polynomials. We set different sizes of calculation domain containing corresponding number of calculation atoms and record the calculation time by serial program. From the Fig. 6 we can see that the calculation time increasing linearly with the number of atoms, namely the calculation time is $\mathcal{O}(N)$.

6 Conclusions

In this paper, we have proposed a linear scaling discontinuous Galerkin density matrix minimization algorithm for finding the ground state energy using the K-S wave ap-

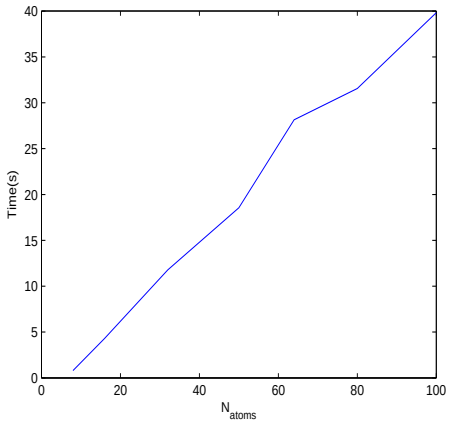

Figure 6: Calculation time with different numbers of calculation atoms.

proach. The key result in this work is the use of physics-based local orbital enriched finite element basis with discontinuous Galerkin method to approximate the support functions for the representation of density operators. It is found that the physics based local orbitals allows the use of coarse finite element mesh, resulting in a compact and efficient discretization of the energy functional in the DMM method. The DG method using this hybrid basis ensures both numerical convergence and efficient capturing of the main structure of the wave functions as shown by numerical tests on simple 1-D lattice systems, where linear scaling performance of the DG-DMM method is also shown. Work is under way to extend the results for the model system to self-consistent computation of electronic structure, especially for 3-D many electron systems.

Acknowledgments

The second and third authors acknowledge the support of U.S. Army Research Office (grant number W911NF-11-1-0364) for this work and the first author thanks the support of NSFC (grant number 11011130029) and of SRF for ROCS, SEM. The authors appreciate the productive discussions with Prof. Weinan E and Drs. J.F. Lu and L. Lin on this work.

References

[1] R. Abgrall and C.-W. Shu. Development of residual distribution schemes for the discontinuous Galerkin method: The scalar case with linear elements. Commun. Comput. Phys., 5(2-4):376–390, 2009.

[2] J.E. Akin. The generation of elements with singularities. Int. J. Numer. Meth. Engng., 10:1249–1259, 1976.

[3] I. Babuška and B. Rosenzweig. A finite element scheme for domains with corners. Numer. Math., 20:1–21, 1972.

[4] J.R. Chelikowsky, N. Troullier, and Y. Saad. Finite difference-pseudopotential method: Electronic structure calculations without a basis. Phys. Rev. Lett., 72:1240–1243, 1994.

[5] B. Cockburn and C.-W. Shu. The local discontinuous galerkin method for time-dependent convection-diffusion systems. SIAM Journal on Numerical Analysis, 35(6):2440–2463, 1998.
[6] Giulia Galli. Linear scaling methods for electronic structure calculations and quantum molecular dynamics simulations. Current Opinion in Solid State and Materials Science, 1(6):864–874, 1996.
[7] Giulia Galli and Michele Parrinello. Large scale electronic structure calculations. Phys. Rev. Lett., 69(24):3547–3550, Dec 1992.
[8] C. J. García-Cervera. A remark on an efficient real space method for orbital-free density-functional theory. Commun. Comput. Phys., 1(1):1–5, 2006.
[9] C. J. García-Cervera. An efficient real space method for orbital-free density-functional theory. Commun. Comput. Phys., 2(2):334–357, 2007.
[10] C.J. García-Cervera, J. Lu, Y. Xuan, and W. E. Linear-scaling subspace-iteration algorithm with optimally localized nonorthogonal wave functions for kohn-sham density functional theory. Phys. Rev. B, 79:115110, 2009.
[11] S. Goedecker. Low complexity algorithms for electronic structure calculations. J. Comput. Phys., 118:261–268, 1995.
[12] S. Goedecker. Linear scaling electronic structure methods. Rev. Mod. Phys., 71(4):1085–1123, Jul 1999.
[13] S. Goedecker and L. Colombo. Efficient linear scaling algorithm for tight-binding molecular dynamics. Phys. Rev. Lett., 73:122–125, Jul 1994.
[14] E. Hernández and M. J. Gillan. Self-consistent first-principles technique with linear scaling. Phys. Rev. B, 51(15):10157–10160, Apr 1995.
[15] W. Kohn and L. J. Sham. Self-consistent equations including exchange and correlation effects. Phys. Rev., 140:A1133–A1138, Nov 1965.
[16] X.-P. Li, R. W. Nunes, and David Vanderbilt. Density-matrix electronic-structure method with linear system-size scaling. Phys. Rev. B, 47(16):10891–10894, Apr 1993.
[17] L. Lin, J. Lu, L. Ying, and W. E. Adaptive local basis set for kohn-sham density functional theory in a discontinuous galerkin framework I: Total energy calculation. submitted to J. Comput. Phys., 2011.
[18] T. Lu and W. Cai. A fourier spectral-discontinuous galerkin method for time-dependent 3-d schrödinger-poisson equations with discontinuous potentials. J. Comput. Appl. Math., 220:588–614, October 2008.
[19] D. Luenberger and Y. Ye. Linear and Nonlinear Programming. Springer, third edition, 2008.
[20] R. Martin. Electronic Structure: Basic Theory and Practical Methods. Cambridge Univ. Press, Cambridge, 2004.
[21] F. Mauri, G. Galli, and R. Car. Orbital formulation for electronic-structure calculations with linear system-size scaling. Phys. Rev. B, 47(15):9973–9976, Apr 1993.
[22] R. McWeeny. The density matrix in self-conssitent field theory. I. iterative constructon of the density matrix. Proc. Roy. Soc. Lond. A, 235:496–509, 1956.
[23] J.C. Slater. Wave functions in a periodic potential. Phys. Rev., 51:846–851, 1937.
[24] N. Troullier and José Luriaas Martins. Efficient pseudopotentials for plane-wave calculations. Phys. Rev. B, 43:1993–2006, Jan 1991.
[25] W. Wang and C.-W. Shu. The wkb local discontinuous Galerkin method for the simulation of Schrödinger equation in a resonant tunneling diode. J. Scientific Computing, 40:360–374, 2009.
[26] W. Yang. Direct calculation of electron density in density-functional theory. Phys. Rev. Lett., 66:1438–1441, Mar 1991.